Thermochimica Acta, 112 (1987) 51–56
Elsevier Science Publishers B.V., Amsterdam – Printed in The Netherlands

CALIBRATION AND APPLICATION OF A "HEAT FLUX DSC" IN THE STUDY OF HETEROGENEOUS CATALYZED REACTIONS

H. Dötsch, H. Fink

Institute of Reactor Components, KFA Jülich, 5170 Jülich, FRG

SUMMARY

The advantages of the heat flux DSC in measuring the reaction rates on catalysts are to be found in a time-saving and economical experimental procedure. The disadvantages result from the indirect reaction rate measurement and the calibration problems. Thus, for example, the calibration factor changes if the reaction-induced thermal conductivity of the ambient gas is changed. Furthermore, when studying "large" specimens in the DSC, the heat exchange between the specimen and gas must be considered.

It is shown that the influence of the measuring system on the calibration factor can be calculated; the influence of the specimen can be determined with the aid of a suitable calibration experiment. The possibilities and limitations of the measuring procedure are demonstrated by the example of methanation and methanol synthesis.

INTRODUCTION

The application of a heat flux DSC for reaction kinetic measurements on catalysts provides a number of advantages in comparison to conventional laboratory reactors. The specimen masses and gas fluxes required are small and "scanning operation" enables the experimental times to be kept very short.

These advantages are contrasted with increased calibration efforts

- if the gas atmosphere in the measuring cell is changed due to experimental conditions and
- if "large" specimens are used.

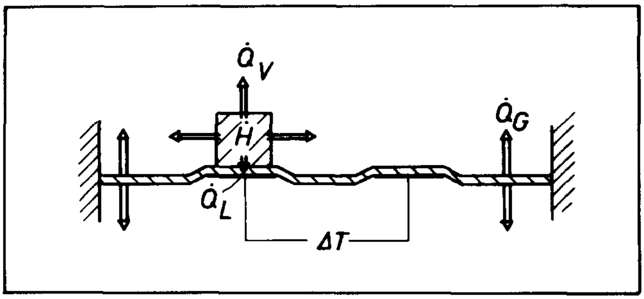

Fig. 1: Heat fluxes in the DSC cell influencing the signal

0040-6031/87/$03.50

This is clearly shown in Fig. 1. The principal component of the DSC cell used by us is a constantan disk, shown here in cross section, equipped with a specimen and reference plateau. The measuring signal is the temperature difference ΔT between these two plateaus. The calibration process now involves linking the measuring signal ΔT to the heat flux $\dot{H}$ generated or consumed in the specimen. Fig. 1 shows qualitatively the heat fluxes of significance for the calibration by the example of an exothermal reaction. Starting from the specimen, heat flows towards the measuring plate ($\dot{Q}_L$) and to the gas ($\dot{Q}_V$). If the specimen is sufficiently small and contact to the measuring plate good then specimen cooling on the gas side is negligible. The heat flux $\dot{Q}_L$ introduced into the measuring plate now flows towards the temperature-regulated cell casing. In this way heat is released to the ambient gas ($\dot{Q}_G$). It can be easily seen that the latter value is influenced, for example, by the thermal conductivity of the cell atmosphere.

We thus have two processes with an attenuating effect: for the same exothermal event, the measuring signal ΔT is at a maximum if the heat fluxes $\dot{Q}_V$ and $\dot{Q}_G$ are negligibly small (small specimen, low thermal conductivity of the cell atmosphere). In the case of an increasing exchange of heat from the measuring plate and specimen with the gas, ΔT decreases with a constant reaction heat flux.

CALIBRATION

This can be illustrated by the temperature profile of the measuring plate. Fig. 2 is the result of a calculation of heat transport in the measuring plate under idealized conditions. The calculation is based on a two-dimensional stationary model with a homogeneous heat source or heat sink.

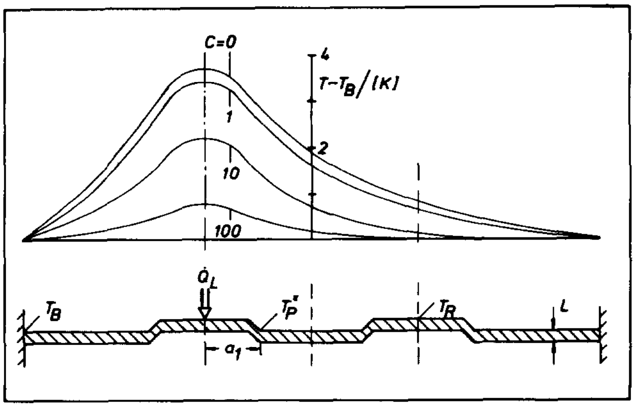

Fig. 2: Temperature course in a section of the measuring plate (ref. 2)

For the region of the specimen plateau we get

$$\frac{\partial^2 (T - T_B)}{\partial (\frac{x}{a_2})^2} + \frac{\partial^2 (T - T_B)}{\partial (\frac{y}{a_2})^2} - C (T - T_B) = - \frac{\dot{Q}_L}{\lambda_C L \pi} (\frac{a_2}{a_1})^2$$

and for the remaining surface of the measuring plate, neglecting the reference specimen,

$$\frac{\partial^2 (T - T_B)}{\partial (\frac{x}{a_2})^2} + \frac{\partial^2 (T - T_B)}{\partial (\frac{y}{a_2})^2} - C (T - T_B) = 0$$

with the dimensionless parameter of plate cooling

$$C = \frac{\lambda_G a_2^2}{\lambda_C L} (\frac{1}{d_1} + \frac{1}{d_2}).$$

The temperature profiles shown in Fig. 2 result for different ambient conditions in the cell for a heat flux $\dot{Q}_L$ of 28 mW introduced into the measuring plate on the specimen side. If no heat is exchanged with the gas then we obtain the envelope of the group of curves (C=0) shown in Fig. 2. In this case, ΔT takes on a maximum value. The value C = 0.73 results for the indium melt in an argon atmosphere and in a hydrogen environment with thermal conductivity 10 times as great it follows C = 7.53.

The calibration factor K can now be calculated via the value of C. If all the reaction heat flows off via the measuring plate ($\dot{H} = \dot{Q}_L$) then the calibration task is thus solved. It was demonstrated on the basis of melt experiments that in the case of "small" specimens with high thermal conductivity in gases of low thermal conductivity that this condition is approximately fulfilled (ref. 2).

However, in the experiments carried out by us we were dealing with relatively large cylindrical catalyst pellets (diameter and height: 4 mm). Not all the reaction heat was transported off via the measuring plate; a considerable fraction was transferred directly to the ambient gas. This fraction designated $\dot{Q}_V$ in Fig. 1, is not of course present in the measuring signal.

In order to take into consideration the effect of direct specimen cooling we have defined the value $F = \dot{Q}_L/\dot{H}$ which describes the fraction of reaction heat reaching the measuring plate.

Several paths are conceivable for determining F:

1) calibration with an inert specimen of known specific heat capacity in the reaction gas
2) calibration with a catalyst specimen of known specific heat capacity in an inert gas of the same conductivity (Ar-He mixture)

3) computational determination of F assuming suitable heat transfer conditions at the specimen.

In the present paper we decided on the first method. It became apparent that the value F was essentially influenced by the specimen geometry as well as by the conductivity of the reaction gas. In contrast to K, F is only slightly temperature-dependent.

APPLICATION

We thus obtain the following as the conditional equation for the released reaction heat $\dot{H}$

$$\dot{H} = \frac{K}{F} \Delta T$$

The conversion rate can be determined from this reaction heat at a known molar formation enthalpy of the reaction studied. If two reactions are possible leading to the same product, then the DSC experiments provide an upper and lower limit for the product yield as illustrated in Fig. 3 by the example of methanation.

$$CO + 3H_2 = CH_4 + H_2O + 206\ \text{kJ/mol}$$
$$CO_2 + 4H_2 = CH_4 + 2H_2O + 165\ \text{kJ/mol}$$

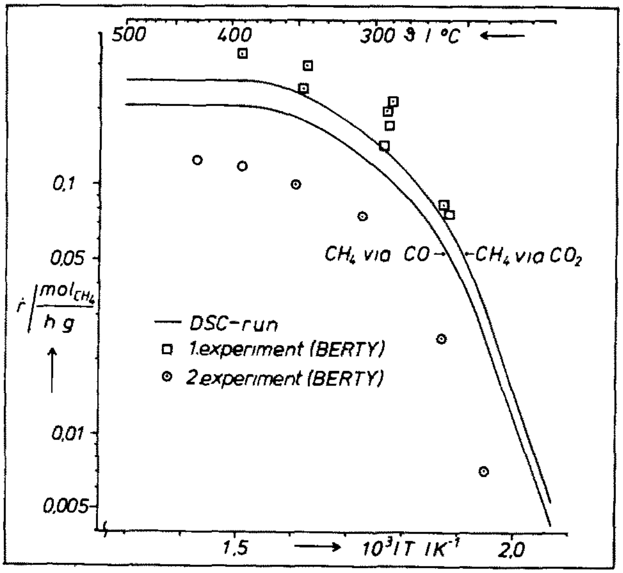

Fig. 3: Arrhenius diagram of methane yield

The experiments were carried out with a reaction mixture containing 10 vol.% CO, 10 vol.% CO_2 and 80 vol.% H_2. The fresh catalyst was first examined in a stirred tank reactor of the Berty type, one pellet was then subsequently studied in the DSC before the pre-aged catalyst batch was subjected once again to conditions in the stirred tank reactor.

The reaction rates thus determined in the DSC led to a detailed reaction model based on the experience of Coenen et al. (ref. 3).

The DSC also provided useful results for methanol synthesis, at least in the range of low CO_2 concentrations.

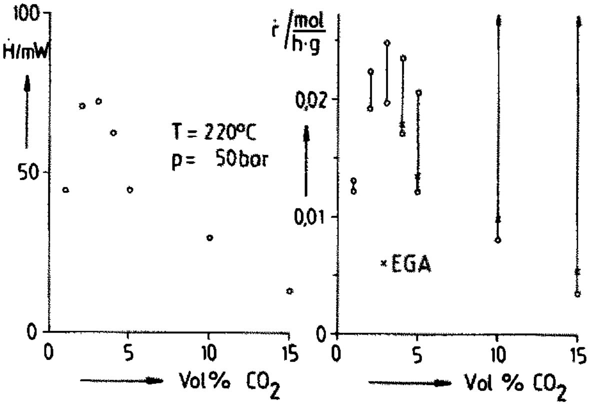

Fig. 4: CO_2 influence in methanol synthesis

In methanol synthesis with Cu/ZnO catalysts, there is a maximum yield with respect to the addition of CO_2 in the reaction gas. This effect has already been described by Klier et al. (ref. 4). Our experiments were all carried out with 80 vol.% H_2, the remainder composed of variable fractions of CO and CO_2. Since even in this case methanol can be formed thermodynamically in two ways

$$CO + 2H_2 = CH_3OH + 91\ kJ/mol$$

$$CO_2 + 3H_2 = CH_3OH + H_2O + 49\ kJ/mol$$

the same problems arise as for methane synthesis. The criterion for the lower boundary of the methanol yield is the exclusive synthesis from CO. The upper boundary was determined via the thermodynamically maximum water content in the product. In the case of high CO_2 contents the two boundaries of the computed methanol yield deviate thus far from each other that an additional evolved gas analysis (EGA) is required.

CONCLUSION

The most important results of our work were as follows:

- The influence of the measuring plate on the calibration factor can be computationally determined.
- The calibration factor can be calculated for "small" and well conducting specimens.
- In the case of the specimens studied by us, the thermal conductivity fraction F was between 0.5 and 0.7.
- The limits of the measuring procedure are reached with high CO_2 concentrations in the methanol synthesis, in this case additional decision-making criteria (evolved gas analysis) are required.

LIST OF SYMBOLS

a_1 (m) - radius of the sample support
a_2 (m) - radius of the measuring plate
C (-) - dimensionless plate cooling parameter
d_1 (m) - space between measuring plate and cover
d_2 (m) - gap below the measuring plate
F (-) - fraction of reaction heat transported to the measuring plate
$\dot{H}$ (W) - reaction heat
K (W/K)- calibration factor for the measuring plate
L (m) - thickness of the measuring plate
T (K) - temperature
T_B (K) - block temperature
ΔT (K) - measuring signal
λ_C (W/mK)- thermal conductivity of the measuring plate
λ_G (W/mK)- thermal conductivity of the gas

REFERENCES

1 G. Hakvoort, L.L. van Reijen, A.J. Aartsen, Measurement of the thermal conductivity of solid substances by DSC, Bratislava, 1985, 8th ICTA

2 H. Dötsch, Bestimmung der Reaktionsgeschwindigkeit an Katalysatorpellets mit einem Wärmeflußkalorimeter, Diss. TH Aachen, 1985, Berichte der Kernforschungsanlage Jülich - JÜL 1989

3 R.Z.C. van Meerten, J.G. Vollenbroeck, M.H.J.M. de Croon, P.F.M.T. Nisselroy, J.W.E. Coenen, The kinetics and mechanism of the methanation of carbon monoxide on a Nickel-Silica catalyst, Journ. of Catalysis, 3 (1982) 29

4 K. Klier, V. Chatikavanij, R.G. Herman, G.W. Simmons, Effect of CO_2 on Methanol Synthesis, Journ. of Catalysis 74 (1982) 343